Inhibitors of myosin, but not actin, alter transport through Tradescantia plasmodesmata. Protoplasma

ARTICLE *in* PROTOPLASMA · JANUARY 2011

Impact Factor: 2.65 · DOI: 10.1007/s00709-010-0244-3 · Source: PubMed

2 AUTHORS, INCLUDING:

Rosemary White
The Commonwealth Scientific and Industri…

68 PUBLICATIONS **2,167** CITATIONS

SEE PROFILE

Protoplasma (2011) 248:205–216
DOI 10.1007/s00709-010-0244-3

ORIGINAL ARTICLE

Inhibitors of myosin, but not actin, alter transport through *Tradescantia* plasmodesmata

Janine E. Radford · Rosemary G. White

Received: 29 August 2010 / Accepted: 10 November 2010 / Published online: 27 November 2010

Abstract Actin and myosin are components of plasmodesmata, the cytoplasmic channels between plant cells, but their role in regulating these channels is unclear. Here, we investigated the role of myosin in regulating plasmodesmata in a well-studied, simple system comprising single filaments of cells which form stamen hairs in *Tradescantia virginiana* flowers. Effects of myosin inhibitors were assessed by analysing cell-to-cell movement of fluorescent tracers microinjected into treated cells. Incubation in the myosin inhibitor, 2,3-butanedione monoxime (BDM) or injection of anti-myosin antibodies increased cell–cell transport of fluorescent dextrans, while treatment with the myosin inhibitor *N*-ethylmaleimide (NEM) decreased cell–cell transport. Pre-treatment with the callose synthesis inhibitor, deoxy-D-glucose (DDG), enhanced transport induced by BDM treatment or injection of myosin antibodies but did not relieve NEM-induced reduction in transport. In contrast to the myosin inhibitors, cell-to-cell transport was unaffected by treatment with the actin polymerisation inhibitor, latrunculin B, after controlling for callose synthesis with DDG. Transport was increased following azide treatment, and reduced after injection of ATP, as in previous studies. We propose that myosin detachment from actin, induced by BDM, opens *T. virginiana* plasmodesmata whereas the firm attachment of myosin to actin, promoted by NEM, closes them.

Keywords Actin · 2,3-Butanedione monoxime (BDM) · Cytochalasin · Cell-to-cell transport · Latrunculin · Myosin · *N*-ethylmaleimide (NEM) · Plasmodesmata · *Tradescantia virginiana*

Handling Editor: Karl Oparka

Electronic supplementary material The online version of this article (doi:10.1007/s00709-010-0244-3) contains supplementary material, which is available to authorized users.

J. E. Radford · R. G. White
Department of Biological Sciences, Monash University,
Melbourne, VIC 3800, Australia

J. E. Radford
Computer Associates,
380 St Kilda Road,
Melbourne, VIC 3004, Australia

R. G. White (✉)
Commonwealth Scientific and Industrial Research Organisation,
Division of Plant Industry,
GPO Box 1600, Canberra, ACT 2601, Australia
e-mail: rosemary.white@csiro.au

Introduction

Molecules can move directly from the cytoplasm of one plant cell into the next if they are connected by plasmodesmata, which are membrane-lined pores through the walls between adjacent cells. They usually allow molecules below a certain size to move from one cell to the next by diffusion but may selectively allow passage of larger molecules, and some permit only one-way traffic of certain molecules (e.g. Tirlapur and König 1999; Kim et al. 2005; Christensen et al. 2009). Simple plasmodesmata are incorporated into new cell walls laid down at cytokinesis and appear to have a common structure, containing a tightly compressed tube of endoplasmic reticulum (ER) ensheathed in a narrow sleeve of cytoplasm, all enclosed within the plasma membrane (reviewed in Roberts and Oparka 2003; Lucas et al. 2009). As plant tissues mature, plasmodesma structure and function are modified, and their permeability is increased or decreased in response to a variety of endogenous and exogenous compounds.

Regulation of permeability remains a mystery, because plasmodesma protein and other regulatory components have not been not fully identified. One regulatory option is via elements of the cytoskeleton, since both actin, and its associated motor protein, myosin, have been found within plasmodesmata (White et al. 1994; Blackman and Overall 1998; Radford and White 1998; Reichelt et al. 1999, reviewed in Aaziz et al. 2001; Oparka 2004). Because actin and myosin are essential elements of the cytoskeleton in all plant cells, at least in the early stages of cell growth and differentiation, we have tended to assume that they regulate all plasmodesmata in the same way.

That this may not be the case includes evidence showing a range of effects of actin filament disrupters in different plant tissues. For example, treatment of *Nephrolepis exaltata* rhizome tips with the actin inhibitor, cytochalasin D, caused plasmodesma widening, seen in transmission electron microscopy (TEM; White et al. 1994), suggesting that actin filament integrity was required to constrain plasmodesmata into narrow channels. Subsequent analyses of cell–cell transport showed that treatment with biochemical or protein inhibitors of actin assembly allowed larger molecules to move between tobacco mesophyll cells (Ding et al. 1996; Su et al. 2010), which concurs with the earlier ultrastructural analysis. However, plasmodesma structure appeared unaffected by cytochalasin D in *Hordeum vulgare* and *Azolla pinnata* root tips (White et al. 1994), and latrunculin B did not increase dye transport across cell boundaries in the well-studied tobacco trichome system (Christensen et al. 2009). Disassembly of actin filaments may result in reduced transport, for example, application of latrunculin B or cytochalasin D (Kawakami et al. 2004; Liu et al. 2005) or local silencing of actin gene expression (Liu et al. 2005) inhibited virus transport between tobacco mesophyll cells.

The role of myosin, the motor protein most commonly associated with actin, has been less well characterised, but the effects of inhibitors also vary with the tissue examined. Volkmann et al. (2003) found that injection of antibodies to the plant-specific myosin VIII increased transport between *Arabidopsis* root epidermis or tobacco mesophyll cells. In contrast, application of the myosin inhibitor, 2,3-butanedione monoxime (BDM) induced neck constrictions in *Zea mays* and *H. vulgare* plasmodesmata measured in TEM (Radford and White 1998), and inhibited intercellular virus transport in tobacco mesophyll tissue (Kawakami et al. 2004). There is no clear explanation for these discrepancies in inhibitor effects, especially since both actin and myosin inhibitors reduced actin–myosin-based cytoplasmic streaming in the tissues examined.

Our aim in the current study was to extend observations of myosin function using a simple system, the filamentous stamen hairs of *Tradescantia virginiana*. Cell–cell transport of fluorescent tracers has been well characterised in this and related systems (Tucker 1982; Tucker et al. 1989; Tucker and Tucker 1993) since it is relatively straightforward to quantify dye movement through a single file of cells of similar dimensions. Their plasmodesmata respond to changes in calcium status and energy level (Tucker 1988, 1990; Tucker and Boss 1996) similarly to those in other higher plant tissues (Erwee and Goodwin 1983; Lew 1994; Holdaway-Clarke et al. 2000), and the actin–myosin cytoskeleton is affected by commonly used inhibitors (Tucker 1987; Salitz and Schmitz 1989; Hepler et al. 2002; Molchan et al. 2002).

As detailed below, we found that cell–cell transport in *T. virginiana* stamen hairs was strongly affected by myosin inhibitors, but was unaffected by the actin polymerisation inhibitor, latrunculin B. We conclude that although *T. virginiana* plasmodesmata may resemble other simple plasmodesmata, their permeability is modified by actin–myosin interactions differently to some previously analysed tissues. This implies that we need to characterise plasmodesma regulation in every tissue type, despite other similarities in their structure and/or regulation, and that the role of the cytoskeleton may vary depending on tissue type and stage of development.

Materials and methods

Plant material

Floral buds of *T. virginiana* L. were obtained, 2–3 days prior to anthesis, from plants grown in an unheated glasshouse in summer in Clayton, Victoria, or grown year-round in a temperature-regulated glasshouse in Canberra, ACT, Australia, and were used immediately in experiments.

Sample preparation

Samples for microinjection were prepared as described previously (Radford and White 2001). Briefly, *T. virginiana* stamens were dissected from a 2–3 mm long floral bud in distilled water using a sharp razor blade and the pollen capsules removed. At this stage, the stamen hairs are still dividing and elongating (e.g. Bonsignore and Hepler 1985), and have simple plasmodesmata in the young walls between adjacent cells (cf. Tucker 1982). The filaments and attached hairs were exposed for 1–2 s to 0.05% Triton X-100 then incubated in various treatment solutions for 45 min before transfer to a chamber slide (described below). Control hairs were bathed in 0.5 mM HEPES (N[2-hydroxyethyl]piperazine-*N*′-[2-ethanesulfonic acid]), 0.1 mM KCl, 0.1 mM $CaCl_2$, 0.1 mM $MgCl_2$, 0.5 mM NaCl pH 7; treated hairs were bathed in this buffer plus

either 2-deoxy-D-glucose (DDG; 0.1 mM), sodium azide (1 mM), BDM (1 mM or 30 mM), *N*-ethylmaleimide (NEM; 1 mM) or latrunculin B (50 nM).

Microinjection procedures

After incubation in treatment solutions, the plant material was mounted horizontally in the well of a chamber slide, as described previously (Radford and White 2001). Specimens were held in place by embedding in a thin layer of 1% ultra low temperature gelling agar (Type IX) that was set by a 5–10 second placement on ice. Fresh treatment solution was immediately added to the wells and the tissues allowed to rest for 15 min prior to microinjection of dye, or dye plus either ATP, adenosine 5′-[γ-thio]-triphosphate (ATPγS), calcium, or anti-myosin antibodies (polyclonal anti-bovine smooth and skeletal myosin; Sigma M7648), thus giving a total of 60 min incubation in the solution.

The range of dyes injected included Lucifer yellow (457.2 Da), sulforhodamine 101 (606.7 Da) and FITC-dextrans of 1–3 kDa and >3 kDa (prepared from polydisperse 4 kDa FITC-dextran). All dyes were used at a concentration of 1 mM in distilled water, and were prepared as described previously (Radford and White 2001).

Unless stated otherwise, the dyes were injected by iontophoresis, in which a brief (1–2 s) negative (Lucifer yellow and sulforhodamine 101) or positive (FITC-dextrans) current was applied down the injection electrode using a current/voltage generator (Model S-7200HV/S-7071A, World Precision Instruments, Sarasota, FL, USA). For pressure injection of the large antibodies, hydraulic pressure was supplied by a 2.0 ml Gilmont syringe (Gilmont Instruments, Extech Equipment, Wantirna South, VIC, Australia) connected via tubing to an Eppendorf micropipette holder (Eppendorf Australia, Sydney, NSW, Australia), as described by Zhang et al. (1990). Only cells in which dyes remained in the cytoplasm were analysed (e.g. Fig. 2); the very few cells in which dye was accidentally injected into the vacuole were discarded, and dyes were never observed in the ER (cf. Electronic supplement material, Fig. 1).

In some experiments, the tissue was injected with either ATP or ATPγS, a non-hydrolysable form of ATP (Islam 1989; Wang et al. 1993). ATP and ATPγS were injected into the cells using a positive current pulse at a tip concentration of 12.5 mM. Since a typical injection introduces a volume less than 1–2% of the cell volume (Tucker and Boss 1996; Radford and White 2001), the final cytoplasmic concentration of ATP or ATPγS would be 0.1–0.2 mM. Calcium was injected together with fluorescent dye (1 mM) at a tip concentration of 10 mM (Erwee and Goodwin 1983), also with a brief positive current.

The antibodies to myosin (stock 5 mg/ml) were diluted 1:10 in distilled water immediately prior to pressure injection. We know that this antibody will bind to plasmodesma myosin as it was used previously to localise the myosin there, and it labelled proteins of the appropriate size on Western blots (Radford and White 1998). The two controls used were boiled anti-myosin, in which the antibody solution was heated to 100°C for 10 min and cooled on ice prior to injection; and myosin+anti-myosin, in which the antibody solution was incubated for 30 min with an equal volume of chicken muscle myosin (5.4 mg/ml) prior to injection.

The larger dyes were scored as moving from the injected cell to the neighbouring cell when fluorescence could be detected in the nucleus and/or cytoplasm. Images were captured via a Panasonic digital video camera mounted onto a Leica DMIRB inverted fluorescence microscope at the time of injection and after 30 min, at which time they

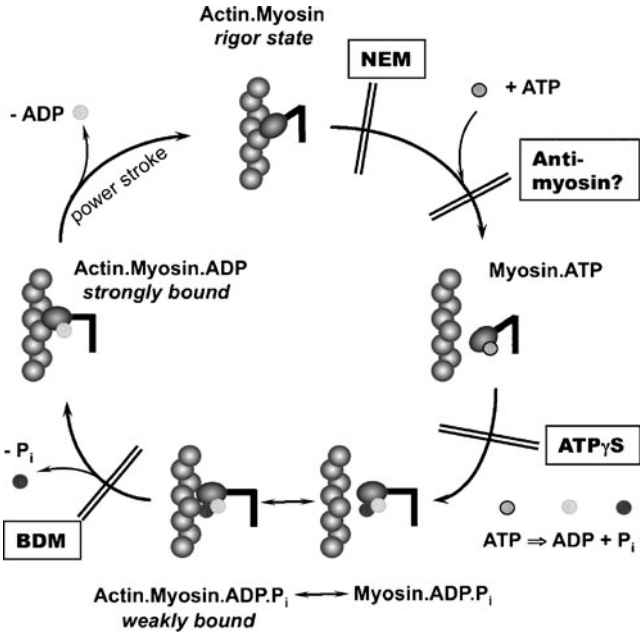

Fig. 1 Diagram showing conformational changes in muscle myosin II during one cycle generating movement (after Spudich 2001), with particular stages thought to be blocked by BDM, NEM and myosin antibodies indicated. **a** In the rigor state, the myosin head is tightly bound to an actin microfilament at an angle of approximately 45° (Uyeda et al. 1996) in the absence of ATP (Cooke 1993). NEM prevents ATP binding to myosin. **b** ATP allows the myosin head to detach from the actin (Mooseker et al. 1991; Spudich 1994). At this stage, anti-myosin antibodies are able to bind to the conserved actin-binding or ATP-binding sites. If ATPγS binds to myosin, it does not undergo hydrolysis. **c** Myosin-bound ATP is rapidly hydrolysed to form myosin.ADP.P_i, during which the myosin head undergoes a conformational change, possibly caused by a hinge-like bending movement between the catalytic domain and regulatory domains in the neck region (Sugimoto et al. 1995), which then allows weak binding to actin. BDM prevents the actin of the myosin ATPase, so prevents ATP hydrolysis. (**d**) The release of P_i generates actin.myosin.ADP, which binds strongly to actin (Cooke 1993; Uyeda et al. 1996). ADP release follows rapidly, with accompanying force-producing movement of the myosin head (Sugimoto et al. 1995), which returns the actin.myosin complex to the initial, tightly bound rigor state (**a**)

were scored as showing transport or not. For the two smallest dyes, the effect of 1 mM BDM on cell-to-cell transport was analysed in more detail, since every injection resulted in transport into at least its immediate neighbour, therefore recording presence or absence of transport was insufficient to distinguish between treatments. After dye injection, the time taken for dye to move up to four cells from the injected cell was recorded and averaged for ten replicate injections in control and treated stamen hairs.

Results

The baseline size exclusion limit (SEL) for *T. virginiana* staminal hair cells was approximately 3 kDa, as determined previously (Radford and White 2001). Pretreatment with the callose synthesis inhibitor, DDG, increased transport and the SEL, and the full effect of DDG was achieved within the first hour of treatment as no further increase in transport was seen after 2 h incubation (Table 1).

Effects of myosin inhibitors

If plant myosins interact with actin and are affected by inhibitors in the same way as other two-headed motor myosins, we can make certain predictions about inhibitor effects on plant actin–myosin interactions. The first inhibitor we used was BDM, which binds directly to myosin in muscle tissue and is thought to arrest the myosin cycle at the myosin.ADP.P_i stage, thus preventing the myosin head from attaching firmly to actin by inhibiting the release of P_i (Fig. 1), although it may inhibit myosin independently of any effects on the actin-activated myosin ATPase (Forer and Fabian 2005). Treatment with 1 mM or 30 mM BDM increased cell-to-cell transport of the 1–3 kDa FITC-dextran (Fig. 2a, b; Table 1), and transport of the >3 kDa FITC-dextran was increased further by incubation with both DDG and BDM (Table 1). Cytoplasmic streaming was slower, but was not completely inhibited by any of these treatments, and cytoplasmic strands remained intact (e.g. Electronic supplementary material, Fig. 2). Since BDM is an oxime derivative, it may also act as a phosphatase (Eisfeld et al. 1997), and could conceivably dephosphorylate plasmodesma proteins and potentially increase cell-to-cell transport (Epel 1994; Fleurat-Lessard et al. 1995). Treatment with ATPγS would prevent any phosphatase activivity, and after pretreatment with BDM, injection of ATPγS decreased transport such that movement of the 1–3 kDa FITC-dextran was completely blocked; even 30 mM BDM appeared unable to prevent closure by ATPγS. Injection of ATP caused transient closure, but after a few seconds, dye transport was similar to that in controls (Table 1).

Table 1 Movement of FITC labelled dextrans in *Tradescantia virginiana* staminal hairs expressed as percentage of injections where transport occurred after the treatments listed below. Dyes were injected by iontophoresis unless otherwise stated; number of injections=10; see "Materials and methods" for treatment details

Treatment	1–3 kDa FITC dextran	>3 kDa FITC-dextran
Control	100	10[a]
0.1 mM DDG (1 h)	–	70
0.1 mM DDG (2 h)	–	70
50 mM DDG (1 h)	–	100[b]
0.1 mM DDG+latrunculin B	–	40
1 mM BDM	–	70
0.1 mM DDG+1 mM BDM	–	100
30 mM BDM	–	80
ATP	100[c]	–
ATPγS	0[d]	–
1 mM BDM+ATPγS	0[d]	–
1 mM NaN_3	–	100
0.1 mM DDG+1 mM NEM	10[e]	–
Control[f]	–	70[e]
Anti-myosin[f]	–	100
Heated anti-myosin[f]	–	60
Calcium	100[g]	–
0.1 mM DDG+calcium	100	100[b]

(–) not tested

[a] Dye spread one to two cells from injected cell within 30 min of injection

[b] Dye transport more rapid than in controls and spread to up to four cells in 30 min

[c] Transport delayed for 3–5 min after injection

[d] No transport by 30 min after injection

[e] Dye spread only to the adjacent cell and was very faint

[f] Dye introduced by pressure injection

[g] Dye spread only to the adjacent cell

Dye movement was followed along cell filaments, and the time taken for Lucifer yellow to move up to four cells from the injected cell after treatment with BDM was not significantly different from the control (Fig. 3). In contrast, the larger dye, sulforhodamine 101, moved the same distance in less than half the time in 1 mM BDM-treated filaments compared with controls (Fig. 3; $p<0.01$ Student's t test). Treatment with DDG prior to incubation in DDG plus BDM reduced this transport time further, to 20% of untreated controls.

The second inhibitor applied was NEM, which has often been used to inhibit actin–myosin-mediated organelle movement and cytoplasmic streaming in plant tissues (Chen and Kamiya 1975; Nagai and Fukui 1981; Dale et al. 1983; Kohno and Shimmen 1988; Menzel 1994; Malec et al. 1996). NEM inhibits the actin-activated myosin ATPase by alkylating two essential sulfhydryl groups in

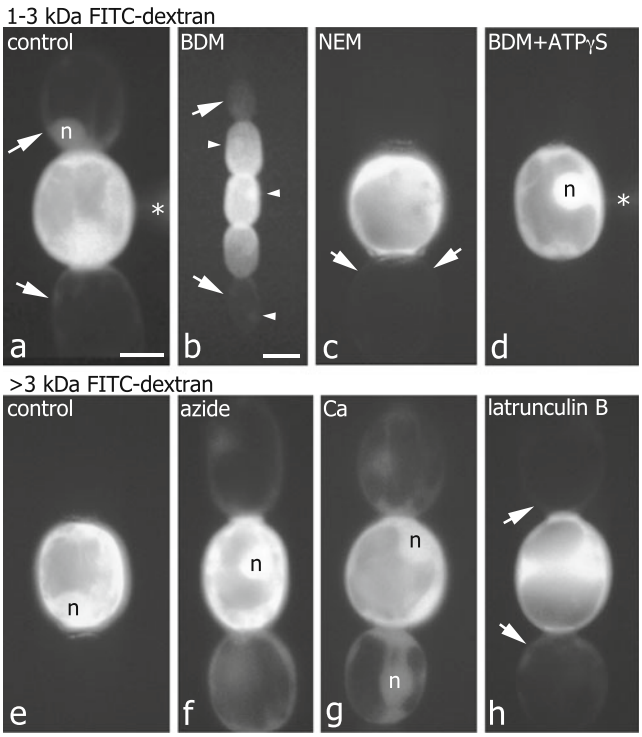

Fig. 2 Fluorescence images of *Tradescantia virginiana* stamen hairs 30 min after injection with 1–3 kDa FITC-dextran (**a**–**d**) or 3 kDa FITC-dextran (**e**–**h**) via iontophoresis following treatment to inhibit myosin or actin function. **a** In untreated stamen hairs, 1–3 kDa FITC-dextran moved into the immediate neighbours (*arrows*). Bar=50 μm; same magnification for (**a**, **c**–**h**). **b** Prior incubation in 1 mM BDM allowed the dye to spread further; the dye was seen faintly in the third cells from the injected cell (*arrows*). Bar=100 μm; small arrowheads indicate fluorescent nuclei. **c** After incubation in 1 mM NEM, this dye was usually confined to the injected cell, and when it was detected in neighbouring cells, was at very low levels (*arrows*). **d** Co-injection of dye with ATPγS after incubation in 1 mM BDM prevented efflux from the injected cell. **e** The 3 kDa FITC-dextran rarely moved out of the injected cell without prior incubation in DDG. **f** Incubation in 1 mM NaN_3 allowed dye efflux to at least one neighbouring cell. **g** After DDG treatment, co-injection of dye with calcium also increased efflux from the injected cell. **h** Even when treatment included DDG, incubation in latrunculin B allowed only slight dye efflux into immediate neighbours (*arrows*). *Asterisk* fluorescence from injection needle; *n* nucleus

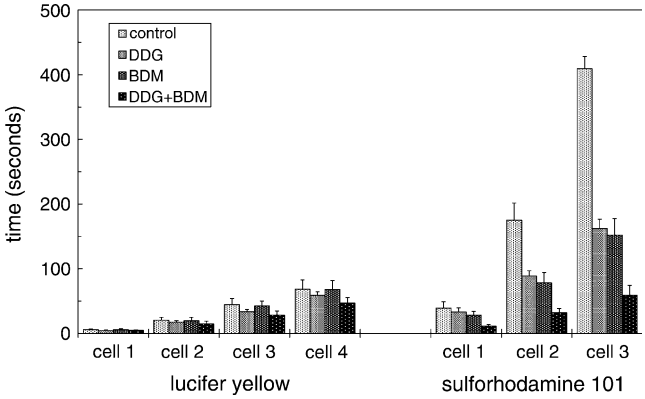

Fig. 3 Time taken (in seconds) for the dyes Lucifer yellow (457.2 Da) or sulforhodamine 101 (606.7 Da) to travel 1, 2, 3 or 4 cells from the injected cell of a *Tradescantia virginiana* stamen hair, with or without prior incubation in 0.1 mM DDG, 10 mM BDM, or 0.1 mM DDG plus 10 mM BDM. *N*=10; *bar*=standard deviation

the head region of the myosin heavy chain, which alters the conformation of the ATP-binding site so that myosin becomes strongly bound to actin in the rigor state (Kohama et al. 1987, Fig. 1). Once in this state, the myosin head cannot be detached from actin by the addition of ATP (Kohama et al. 1987; Patel et al. 1998). Since NEM arrests the actin–myosin cross-bridge cycle such that the myosin head remains firmly attached to the actin filament, opposite to the action of BDM, we predicted that NEM would have the opposite effect on plasmodesmata. Incubation in 1 mM NEM completely inhibited cytoplasmic streaming within 3–4 min of application to the cells (Electronic supplementary material, Fig. 3) and reduced cell–cell transport (Fig. 2c; Table 1). Even after pretreatment of staminal hairs with DDG followed by incubation in DDG plus NEM, transport of the 1–3 kDa FITC-dextran was substantially decreased, and there was no detectable transport of the >3 kDa FITC-dextran (Table 1).

Effects of anti-myosin antibodies

The third, and most specific, inhibition of myosin-based motility was obtained by injection of myosin antibodies (Kiehart et al. 1982; Schindler and Jiang 1986; Zurek et al. 1990; Doberstein et al. 1993; Grolig et al. 1996; Volkmann et al. 2003), which are thought to arrest motility by preventing proper attachment to actin, or by preventing myosin head conformational changes (Doberstein et al. 1993; Grolig et al. 1996), hence arresting it at the myosin. ADP.P_i stage (Fig. 1). We used an antibody which labelled proteins of the appropriate size on Western blots of plant extracts, a subset of which also bound purified rabbit actin (Radford and White 1998). We predicted that anti-myosin antibodies would have the same effect on the SEL as BDM, and co-injection with myosin antibodies did increase transport of the >3 kDa FITC-dextran (Table 1). In addition, the spread of dye was rapid and soon seen up to 4 cells away from the site of injection whereas in the controls, dye spread was minimal and could be seen only faintly in the neighbouring cell. Effects on cytoplasmic streaming appeared gradually; streaming first slowed and organelle movement became erratic and jerky, then eventually all movement ceased.

Changes in energy, phosphorylation and calcium status

In animal cells, BDM can affect intracellular calcium levels (Gyorke et al. 1993; Zhu and Ideka 1993; Xiao and

McArdle 1995; Byron et al. 1996; Ferreira et al. 1997; Allen et al. 1998) so we also tested the effects on cell–cell transport of changing the calcium and energy status of the cells. Cell-to-cell dye transport was not significantly affected by calcium injection, with only slightly reduced transport of the 1–3 kDa FITC-dextran (Table 1), in contrast to previous work in similar systems, in which the overall effect was a reduction in cell–cell transport (Tucker 1990; Tucker and Boss 1996). Pretreatment with DDG not only relieved this slight inhibition of transport (Fig. 2a, g) but subsequent injection of calcium actually increased movement of the >3 kDa FITC-dextran to equal to that seen in the DDG plus BDM treatment (Table 1). As far as we know, this is the first report of calcium injections increasing cell-to-cell transport.

Plasmodesmata are sites of phosphatase activity (Robards and Kidwal 1979; Didhevar and Baker 1986; Chen et al. 1994) of which the actin-activated myosin ATPase is only one potential candidate. In general, phosphorylation of plasmodesmatal protein components is thought to decrease cell-to-cell transport whereas dephosphorylation increases transport (Epel 1994, Fleurat-Lessard et al. 1995), although the specific proteins undergoing phosphorylation and dephosphorylation are not known.

Since ATPγS is a slowly hydrolysed form of ATP which will irreversibly phosphorylate proteins for up to 1 h, we expected it to keep the myosin in the myosin.ATP state (Fig. 1). In muscle tissue, ATPγS caused a complete dissociation of the myosin heads from actin (Roopnarine and Thomas 1996), and in higher plants, phosphorylation decreased actin/myosin-mediated tension in transvacuolar strands of soybean cells (Grabski et al. 1998) also suggesting that the myosin is in the detached state. Hence, we predicted an increase in dye transport after injection of ATPγS, as seen for the detached state myosin treatments (BDM, myosin antibodies) outlined above, with a more transient effect of injected ATP. However, injection of either ATP or ATPγS alone prevented transport of 1–3 kDa FITC-dextran for 3–5 min (ATP) or 25–40 min (ATPγS) (Table 1, Fig. 2d), and both treatments caused a temporary inhibition of streaming. In each case, recovery of cell-to-cell transport occurred at the same time as recommencement of streaming.

Sodium azide is a metabolic inhibitor that decreases cellular ATP levels (Hayashi 1960; Shimmen and Tazawa 1983). In the absence of ATP, endoplasmic organelles were immobilised on actin fibres in green algal cells, and could not be removed by perfusion (Williamson 1975) but could be released after the addition of ATP (Williamson 1992). This suggests that low cell ATP can trap myosin in the rigor state, opposite to the predicted effect of ATPγS, and we would predict decreased cell–cell transport. However, sodium azide increased transport (Table 1; Fig. 2e, f), as seen also in stamen hair cells of *Setcreasea purpurea* (Tucker 1993), and in wheat root cells (Cleland et al. 1994).

High concentrations of DDG have been used extensively in animal systems to inhibit the glycolytic pathway of ATP production (Oiwa et al. 1993; Macri et al. 1995; Brauer et al. 1997). In maize root hair cells, incubation in 50 mM DDG for 180 min caused ATP to decline to 9% of the control (Brauer et al. 1997). We expected this treatment to have similar effects to sodium azide, and although the percentage of injections showing transport was identical after azide or 50 mM DDG treatment, dye injected into cells incubated in 50 mM DDG spread faster and could be detected further from the injected cell (Table 1).

The effects of latrunculin B

Latrunculin B binds to monomeric actin with high affinity, which inhibits polymerisation of new actin microfilaments (Gibbon et al. 1999). In plant cells, this causes depolymerisation of actin microfilaments because the cortical actin network undergoes rapid turnover, certainly in the *Tradescantia* stamen hair system (e.g. Molchan et al. 2002), and the overall effect of latrunculin B is to disrupt actin organisation (e.g. Vidali et al. 2001). If the actin in plasmodesmata is susceptible to degradation by latrunculin B treatment, we should detect an effect on cell–cell transport. Incubation in 1 mM latrunculin B inhibited streaming within the stamen hair cells within 1 h (Electronic supplementary material, Fig. 4), and caused breakdown of the transvacuolar strands. These effects were completely reversible, with recovery of streaming by 1 h after washout. Cell-to-cell transport in the DDG plus latrunculin B treatment was similar to that in the DDG only treatment (Fig. 2h; Table 1).

Discussion

Myosin function is required for cell–cell transport

Transport between *T. virginiana* cells was clearly affected by inhibitors of myosin function. Inhibitors of animal myosins generally have similar effects on plant myosins, and the actin-binding region of the myosin head and actin–myosin interaction are highly conserved across kingdoms (El-Mezgueldi and Bagshaw 2008; Holmes 2008; Yamamoto 2008). We predicted that BDM or anti-myosin antibodies would cause myosin detachment from actin (see Fig. 1), and if this prediction is correct for actin–myosin interactions in *T. virginiana* stamen hairs, then myosin detachment opens plasmodesmata. In an earlier study, Kawakami et al. (2004) found that although BDM reduced intracellular movement within tobacco mesophyll cells, they could still detect cell–cell virus transport after 3 h, and the diameter of the

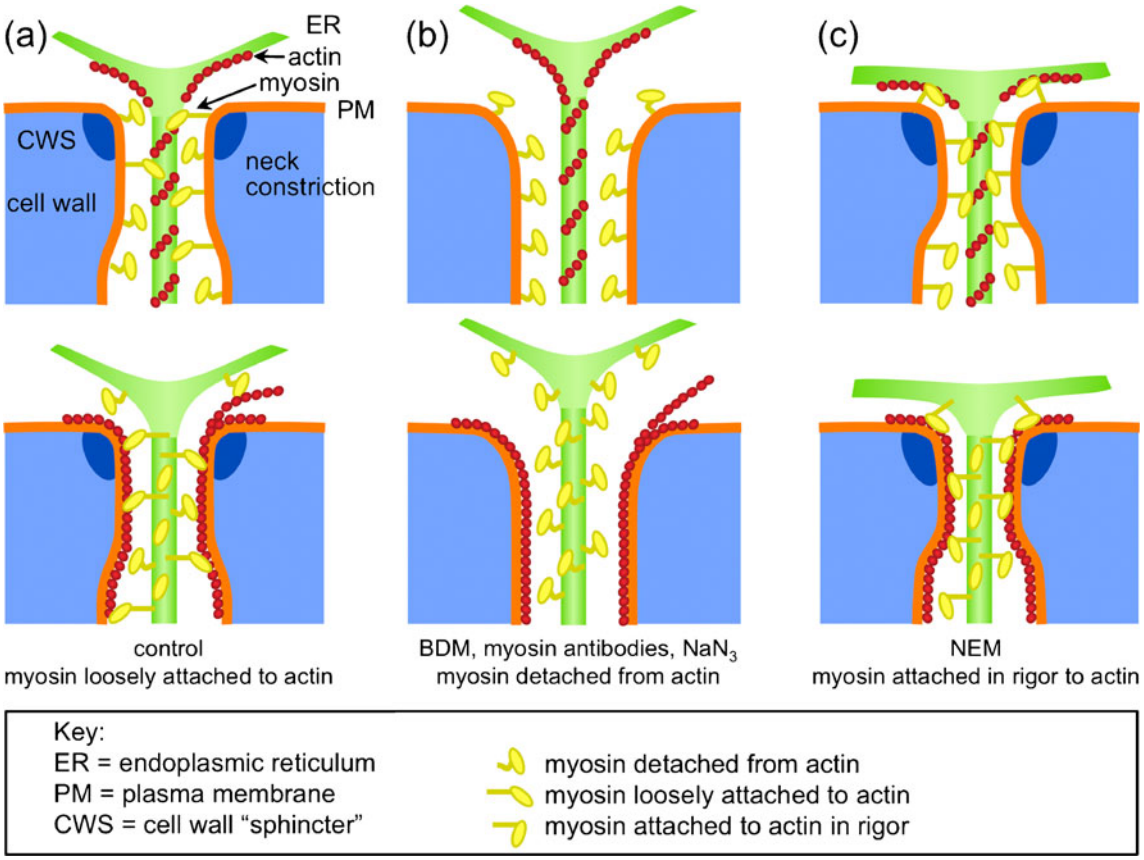

Fig. 4 Diagram suggesting possible actin and myosin conformations to explain responses of *Tradescantia virginiana* plasmodesmata to applied actin–myosin inhibitors. **a** In untreated cells, myosin may adopt a variety of conformations, with loose binding of ER to plasma membrane via a proportion of myosin bound to actin, whether it lines the ER (*top*) or plasma membrane (*bottom*). **b** After BDM treatment, injection of anti-myosin antibodies, or incubation with sodium azide, myosin is completely detached from actin, enlarging the cytoplasmic pathway, especially at the neck region. **c** After NEM treatment, myosin is locked onto actin in rigor, and closes the neck passage more than in control cells

multicellular fluorescent infected areas was not significantly different from controls, which appears different to our results. Prokhnevsky et al. (2005) also found that granules containing a fluorescently tagged viral heat-shock protein not only would not move to plasmodesmata, but were prevented from forming in the presence of BDM. Thus it would appear that components of the cytoskeleton are essential for intracellular assembly and/or movement of some viruses and movement complexes, which makes it difficult to assess effects of cytoskeleton inhibitors on intercellular transport.

The use of BDM as a myosin inhibitor has been criticised in the past, not only because it often has no effect on cytoplasmic streaming unless applied at high concentrations (McCurdy 1999; Forer and Fabian 2005), but also because it may modify other cell processes. For example, BDM has been shown repeatedly to alter calcium influx and efflux through sarcoplasmic reticulum calcium channels (Blanchard et al. 1990; Lang and Paul 1991; Watanabe 1993; Zhu and Ideka 1993; Phillips and Altschuld 1996; Verrucchia and Hervé 1997; Adams et al. 1998), and if plant cells respond similarly, BDM might cause plasmodesma closure by increasing cellular calcium (Erwee and Goodwin 1983; Baron-Epel et al. 1988; Tucker 1990; Lew 1994; Holdaway-Clarke et al. 2000). Since injection of calcium opened plasmodesmata in *T. virginiana* hairs, it was possible that BDM induced opening via increased intracellular calcium. However, Molchan et al. (2002) found that even 30 mM BDM did not increase cell calcium in *T. virginiana* stamen hair cells, therefore it is unlikely that BDM affects plasmodesmata by this mechanism. Finally, Forer and Fabian (2005) in a comprehensive review concluded that BDM is a reasonably specific inhibitor of myosin function, and it has been shown to inhibit *Chara corallina* myosin XI (Funaki et al. 2004). Nevertheless, it remains to be elucidated exactly how BDM interacts with higher plant myosins VIII and XI.

Regulation of plasmodesmata by protein phosphorylation has been discussed many times as plasmodesmata are sites of phosphatase activity (Robards and Kidwal 1979; Didhevar and Baker 1986; Chen et al. 1994), and blocking

this activity will have effects on proteins other than myosin. In general, phosphorylation of plasmodesmatal protein components leads to a decrease in cell-to-cell transport, as seen here, after treatment with either ATP or ATPγS, while dephosphorylation leads to an increase in transport (reviewed in Epel 1994; Fleurat-Lessard et al. 1995).

Our results support the generally accepted hypothesis that phosphorylation decreases cell–cell transport whereas dephosphorylation increases transport. This suggests that the actin-activated ATPase site on the myosin motor domain may not be the primary target of phosphorylation. Instead, phosphorylation of myosin regulatory domains may activate or deactivate myosin irrespective of the actin-activated ATPase site. While the ATPase activity of plasmodesma-located myosin VIII has not yet been characterised, myosin XI, which is responsible for cytoplasmic streaming, is deactivated by phosphorylation and reactivated by dephosphorylation (Tominga et al. 1987; Williamson 1992).

The myosin in plasmodesmata may be regulated similarly to the unconventional myosin, Nina C, which has a kinase domain completely independent of the motor ATPase domain (Mooseker et al. 1991). In Nina C (a retinal protein), a kinase deletion leads to defects in electrophysiological response to light whereas a myosin deletion leads to retinal degradation (Mermall et al. 1998). It is possible that the myosin in plasmodesmata is part of a signal transduction pathway stimulated by phosphorylation.

For more targetted inhibition, myosin action was blocked with anti-myosin antibodies, which opened *T. virginiana* plasmodesmata, as seen previously in *Arabidopsis* root epidermal cells and tobacco mesophyll cells (Volkmann et al. 2003). Here, we used a polyclonal antibody to heavy and light chains of smooth and skeletal myosin, and we predicted that it might prevent myosin binding to actin by steric inhibition or by occupying the actin-binding site (Fig. 1). Polyclonal antibodies which recognise proteins across kingdoms usually interact with conserved motifs, and for myosin, the actin-binding and ATP-binding epitopes are among the most highly conserved (Holmes 2008). In contrast, the antibody to the unique coiled-coil tail region of plant myosin VIII (Volkmann et al. 2003) presumably interferes with myosin attachment to specific cargo or to membranes rather than preventing binding to actin. Nevertheless, that anti-myosin injection produced similar results to BDM treatment suggests that BDM is not artefactually opening plasmodesmata, for example, by interacting with other cell phosphatases.

In contrast to the effects of BDM or myosin antibodies, we predicted that NEM would cause firm attachment of myosin to actin in the rigor conformation, and if correct, then firm binding of myosin to actin causes plasmodesma closure in *T. virginiana*. NEM also inhibits cell-to-cell transport in *Nitella translucens* (Dale et al. 1983), although cell-to-cell transport in large algal cells is highly dependent on streaming rates (Bostrom and Walker 1976; Zawadzki and Fensom 1986) and Dale et al. (1983) concluded that NEM-induced cessation of streaming was the most likely cause of the observed reduction in transport. In the much smaller stamen hair cells examined here, intracellular diffusion does not appear to restrict intercellular transport (Tucker 1987). The average half-time for recovery of GFP fluorescence after photobleaching in tobacco BY-2 suspension cells was 0.48 s after BDM treatment vs. 0.31 s in conrols (Esseling-Ozdoba et al. 2008), indicating that although diffusion within the cytoplasm was slowed by BDM, this rate is still at least an order of magnitude faster than our current ability to detect cell–cell dye transport.

NEM has been shown to inhibit many systems other than myosin in plants, including an H^+ transporting inorganic phosphatase (Gordon-Weeks et al. 1996), chloroplast amylase (Xiong et al. 1998), H^+ pumps (Vincente and Vale 1994), phosphatidate phosphatase 1 (Furukawa-Stoffer et al. 1998), L-myo-inositol 1-phosphatase synthase (RayChaudhuri et al. 1997), Ca^{2+} and other ion channels (Schumaker and Gizinski 1995; Malec et al. 1996), vacuolar H^+-pyrophosphatase (Zhen et al. 1994) and a Ca^{2+}-dependent proteinase (Safadi et al. 1997). The cysteine residue in animal myosin II which is targetted by NEM is present, in nearly the same position, in the plant myosin class XI family, but is absent from the class VIII myosins (Seki et al. 2003, Yamamoto 2008). Both the motility and ATPase activity of *Chara* myosin XI were reduced by NEM, although much less than in skeletal muscle myosin II (Seki et al. 2003), which suggested that inhibition of other proteins by NEM may have slowed cytoplasmic streaming in *Chara*.

It is unclear how NEM would interact with myosin VIII, the putative plasmodesma myosin (Reichelt et al. 1999); perhaps one or more of the myosin XI family plays some part in regulation of permeability, although none of the fluorescent protein-tagged myosin XI tail regions have localised there to date (Walter and Holweg 2008, Avisar et al. 2009; Reisen and Hanson 2007; Sattarzadeh et al. 2009). When transiently expressed in *Nicotiana tabacum*, three of the four myosin VIII family were detected at the plasma membrane, with the fourth located in the nucleus (Avisar et al. 2009) whereas in *N. benthamiana* leaves, one GFP-fusion with the IQ-tail zone of ATM1 localised to plasmodesmata (Golomb et al. 2008). This suggests that myosin VIII association with plasmodesmata is specific and fairly tightly regulated.

Inhibition of actin polymerisation did not alter cell–cell transport

Previous work had shown that treatment with actin disrupters could either open plasmodesmata (White et al.

1994) and increase cell–cell transport (Ding et al. 1996; Su et al. 2010) or conversely, decrease transport (Kawakami et al. 2004; Liu et al. 2005), or even have no effect on either transport (Christensen et al. 2009) or plasmodesma structure (White et al. 1994). Here, we used one inhibitor of actin polymerisation, latrunculin B, to enable comparison with these earlier results, and observed no effect on cell–cell transport in *T. virginiana*. In experiments investigating whether the rate of cytoplasmic streaming within cells could affect intercellular transport, cytochalasin B also appeared to have little effect on transport of small dyes between cells in both *Elodea canadensis* (Erwee and Goodwin 1983) and *S. purpurea* (Tucker 1987). Since myosin inhibitors did affect cell–cell transport in *T. virginiana*, we assume actomyosin plays some role, but suggest that actin may be strongly cross-linked in stamen hair plasmodesmata, and not susceptible to agents which depolymerise the actin cytoskeleton, at least at the concentrations that inhibit streaming. That high concentrations of proteases were needed to degrade plasmodesmata (Tilney et al. 1991; Turner et al. 1994) implies some stabilisation of plasmodesmatal proteins. Furthermore, whereas plant actin filaments are generally difficult to preserve for TEM by chemical fixation, many TEM images of plasmodesmata consistently show globular structures, interpreted to be proteins, within the cytoplasmic sleeve. If some of these structures are actin in polymeric form, then it is relatively stable, perhaps like the stable cortical actin filaments retained on tobacco membrane ghosts (Collings et al. 1998). One stabilising agent is likely to be tropomyosin, which appears to be located specifically at plasmodesmata (Faulkner et al. 2009). Cytochalasin treatment induced more open plasmodesmata only in very young, recently divided cells in one of four tissues examined (White et al. 1994) or after pressure injection of dyes and other compounds (Ding et al. 1996; Su et al. 2010) and it seems likely that a combination of tissue type and mode of analysis produces unique results.

Myosin regulation of plasmodesma permeability

If the predictions in Fig. 1 are correct for effects of inhibitors on plasmodesma myosin, then in *T. virginiana*, detached myosin leads to open plasmodesmata, while tight attachment of myosin to actin results in closed plasmodesmata. One way to explain this behaviour would see the outer plasma membrane compressed into the cell wall if it became separated or detached from the inner strand of ER, creating a wider cytoplasmic channel, especially at the neck region, thus allowing traffic of larger molecules (Fig. 4b). In *N. exaltata* tissue, cytochalasin B not only opened plasmodesma neck regions but also eliminated external material at the neck (White et al. 1994), and we have assumed the same might happen in tissue treated with plasmodesma-opening myosin inhibitors. This mechanism assumes that myosin tails are inserted into one of the membranes whereas actin is bound to the other membrane, with the cytoplasmic channel running between. Hence, when at least some of the myosin is attached to actin, the plasma membrane and ER are held a certain distance apart and the plasmodesmata are less open (Fig. 4a), with even greater restriction of transport obtained by contraction of the myosin head into the rigor conformation, narrowing cytoplasmic channels further (Fig. 4c).

Concluding remarks

We aimed to clarify the role of the cytoskeleton in plasmodesmata, particularly the role of myosin, by analysing a simple system, a single file of cells containing walls with simple plasmodesmata with well-characterised responses to changes in energy status, calcium level and actin integrity. Our results show that myosin also plays a key role in the regulation of cell-to-cell transport through plasmodesmata, but we suggest that this role may be largely structural, maintaining the permeability at the neck region, rather than motile, and actively transporting cargo from cell to cell. Evidence presented here and in previous work shows a range of responses to myosin motility inhibitors, suggesting that myosin function in plasmodesmata is likely to be species- and/or tissue-specific.

We now conclude that we have instead clarified the behaviour of plasmodesmata in a specific tissue type at a particular stage of development. It is clear that we need more detailed information about the structure and function of the cytoskeleton associated with plasmodesmata in a range of plant tissues through development.

Acknowledgements This research was supported by the Australian Research Council (RW) and by an Australian Postgraduate Student Award (JR).

Conflicts of interest The authors declare that they have no conflicts of interest.

References

Aaziz R, Dinant S, Epel BL (2001) Plasmodesmata and plant cytoskeleton. Trends Plant Sci 6:326–330

Adams W, Trafford AW, Eisner DA (1998) 2, 3-Butanedione monoxime (BDM) decreases sarcoplasmic reticulum Ca content by stimulating Ca release in isolated rat ventricular myocytes. Pflügers Archiv Eur J Physiol 436:776–781

Allen TJ, Mikala G, Wu X, Dolphin AC (1998) Effects of 2,3-butanedione monoxime (BDM) on calcium channels expressed in *Xenopus* oocytes. J Physiol 508:1–14

Avisar A, Abu-Abied M, Belausov E, Sadot E, Hawes C, Sparkes IA (2009) A comparative study of the involvement of 17 *Arabidopsis*

myosin family members on the motility of Golgi and other organelles. Plant Physiol 150:700–709
Baron-Epel O, Hernandez D, Jiang L-W, Meiners S, Schindler M (1988) Dynamic continuity of cytoplasmic and membrane compartments between plant cells. J Cell Biol 106:715–721
Blackman LM, Overall RL (1998) Immunolocalisation of the cytoskeleton to plasmodesmata of *Chara corallina*. Plant J 14:733–741
Blanchard EM, Smith GL, Allen DG, Alpert NR (1990) The effects of 2,3-butanedione monoxime on initial heat, tension, and aequorin light output of ferret papillary muscles. Pflügers Arch 416:219–221
Bonsignore CL, Hepler PK (1985) Caffeine inhibition of cytokinesis: dynamics of cell plate formation-deformation in vivo. Protoplasma 129:28–35
Bostrom TE, Walker NA (1976) Intercellular transport in plants. II. Cyclosis and the rate of intercellular transport of chloride in Chara. J Exp Bot 27:347–357
Brauer D, Uknalis J, Triana R, Shachar-Hill Y, Tu S-I (1997) Effects of bafilomycin A, and metabolic inhibitors on the maintenance of vacuolar acidity in maize root hair cells. Plant Physiol 113:809–816
Byron KL, Puglisi JL, Holda JR, Eble D, Samarel AM (1996) Myosin heavy chain turnover in cultured neonatal rat heart cells: effects of $[Ca^{2+}]I$ and contractile activity. Amer J Physiol 271:C1447–C1456
Chen JC, Kamiya N (1975) Localization of myosin in the internodal cell of *Nitella* as suggested by differential treatment with *N*-ethylmaleimide. Cell Struct Funct 1:1–9
Chen S, Das P, Hari V (1994) In situ localization of ATPase activity in cells of plants infected by maize dwarf mosaic potyvirus. Arch Virol 134:433–439
Christensen NM, Faulkner CR, Oparka K (2009) Evidence for unidirectional flow through plasmodesmata. Plant Physiol 150:96–104
Cleland RE, Fujiwara T, Lucas WJ (1994) Plasmodesmal-mediated cell-to-cell transport in wheat roots is modulated by anaerobic stress. Protoplasma 178:81–85
Collings DA, Asada T, Allen NS, Shibaoka H (1998) Plasma membrane-associated actin in Bright Yellow 2 tobacco cells. Plant Physiol 118:917–928
Cooke R (1993) The actomyosin engine. FASEB J 9:636–642
Dale N, Lunn G, Fensom DS (1983) Rates of axial transport of ^{11}C and ^{14}C in *Characean* cells: faster than visible streaming? J Exp Bot 34:130–143
Didhevar F, Baker DA (1986) Localization of ATPase in sink tissue of *Ricinus*. Ann Bot 57:823–828
Ding B, Kwon M-O, Warnberg L (1996) Evidence that actin filaments are involved in controlling the permeability of plasmodesmata in tobacco mesophyll. Plant J 10:157–164
Doberstein SK, Baines IC, Wiegand G, Korn ED, Pollard TD (1993) Inhibition of contractile vacuole function *in vivo* by antibodies against myosin-I. Nature 365:841–843
Eisfeld J, Mikala G, Varadi G, Schwartz A, Klockner U (1997) Inhibition of cloned human L-type cardiac calcium channels by 2, 3-butanedione monoxime does not require PKA-dependent phosphorylation sites. Biochem Biophys Res Commun 230:489–492
El-Mezgueldi M, Bagshaw CR (2008) The myosin family: biochemical and kinetic properties. In: Coluccio LM (ed) Chapter 3 Myosins: a superfamily of molecular motors. Springer, New York, pp 55–93
Epel BL (1994) Plasmodesmata: composition, structure and trafficking. Plant Mol Biol 26:1343–1356
Erwee MG, Goodwin PB (1983) Characterisation of the *Egeria densa* planch. leaf symplast. Inhibition of the intercellular movement of fluorescent probes by group II ions. Planta 158:320–328
Esseling-Ozdoba A, Houtman D, van Lammeren AAM, Eiser E, Emons AMC (2008) Hydrodynamic flow in the cytoplasm of plant cells. J Microsc 231:274–283
Faulkner CR, Blackman LM, Collings DA, Cordwell SJ, Overall RL (2009) Anti-tropomyosin antibodies co-localise with actin microfilaments and label plasmodesmata. Eur J Cell Biol 88:357–369
Ferreira G, Artigas P, Pizarro G, Brum G (1997) Butanedione monoxime promotes voltage-dependent inactivation of L type calcium channels in heart. Effects on gating currents. J Mol Cell Cardiol 29:777–787
Fleurat-Lessard P, Bouché-Pillon S, Leloup C, Lucas WJ, Serrano R, Bonnemain J-L (1995) Absence of plasma membrane H^+-ATPase in plasmodesmata located in pit-fields of the young reactive pulvinus of *Mimosa pudica* L. Protoplasma 188:180–185
Forer A, Fabian L (2005) Does 2,3-butanedione monoxime inhibit nonmuscle myosin? Protoplasma 225:1–4
Funaki K, Nagata A, Akimoto Y, Shimada K, Ito K, Yamamoto K (2004) The motility of *Chara corallina* myosin was inhibited reversibly by 2,3-butanedione monoxime (BDM). Plant Cell Physiol 45:1342–1345
Furukawa-Stoffer T, Byers SD, Hodges DM, Laroche A, Weselake RJ (1998) Identification of *N*-ethylmaleimide-sensitive and -insensitive phosphatidate phosphatase activity in microspore-derived cultures of oilseed rape. Plant Sci 131:139–147
Gibbon BC, Kovar DR, Staiger CJ (1999) Latrunculin B has different effects on pollen germination and tube growth. Plant Cell 11:2349–2363
Golomb L, Abu-Abied M, Belausov E, Sadot (2008) Different subcellular localizations and functions of *Arabidopsis* myosin VIII. BMC Plant Biol 8:3
Gordon-Weeks R, Steele SH, Leigh RA (1996) The role of magnesium, pyrophosphate, and their complexes as substrates and activators of the vacuolar H^+-pumping inorganic pyrophosphatase. Plant Physiol 111:195–202
Grabski S, Arnoys E, Busch B, Schindler M (1998) Regulation of actin tension in plant cells by kinases and phosphatases. Plant Physiol 116:279–290
Grolig F, Schroder J, Sawitzky H, Lange U (1996) Partial characterization of a putative 110 kDa myosin from the green alga *Chara corallina* by *in vitro* binding of fluorescence F-actin. Cell Biol Int 20:365–373
Gyorke S, Dettbarn C, Palade P (1993) Potentiation of sarcoplasmic reticulum Ca^{2+} release by 2,3-butanedione monoxime in crustacean muscle. Pflügers Arch 424:39–44
Hayashi T (1960) Experimental studies on protoplasmic streaming in Characeae. Sci Pap Coll Gen Educ Univ Tokyo 10:245–282
Hepler PK, Valster A, Molchan T, Vos JW (2002) Roles for kinesin and myosin during cytokinesis. Philos Trans R Soc Lond B 357:761–766
Holdaway-Clarke TL, Walker NA, Hepler PK, Overall RL (2000) Physiological elevations in cytoplasmic free calcium by cold or ion injection result in transient closure of higher plant plasmodesmata. Planta 210:329–335
Holmes KC (2008) Myosin structure. In: Coluccio LM (ed) Chapter 2 in Myosins: a superfamily of molecular motors. Springer, New York, pp 35–54
Islam K (1989) Thylakoid protein phosphorylation and associated photosystem II fluorescence changes: a study with the ATP analogue adenosine-5-*O*-thiotriphosphate (ATPγS). Biochim Biophys Acta 974:267–273
Kawakami S, Watanabe Y, Beachy RN (2004) Tobacco mosaic virus infection spreads cell to cell as intact replication complexes. Proc Natl Acad Sci USA 101:6291–6296
Kiehart DP, Mabuchi I, Inoué S (1982) Evidence that myosin does not contribute to force production in chromosome movement. J Cell Biol 94:165–178

Kim I, Kobayashi K, Cho E, Zambryski PC (2005) Subdomains for transport via plasmodesmata corresponding to the apical–basal axis are established during *Arabidopsis* embryogenesis. Proc Natl Acad Sci USA 102:11945–11950

Kohama K, Kohama T, Kendrick-Jones J (1987) Effect of *N*-ethylmaleimide on Ca-inhibition of *Physarum* myosin. J Biochem 102:17–23

Kohno T, Shimmen T (1988) Mechanism of Ca^{2+} inhibition of cytoplasmic streaming in lily pollen tubes. J Cell Sci 91:501–509

Lang RJ, Paul RJ (1991) Effects of 2,3-butanedione monoxime on whole-cell Ca^{2+} channel currents in single cells of the guinea-pig taenia caeci. J Physiol 433:1–23

Lew RR (1994) Regulation of electrical coupling between *Arabidopsis* root hairs. Planta 195:67–73

Liu J-Z, Blancaflor EB, Nelson RS (2005) The Tobacco mosaic virus 126-kilodalton protein, a constituent of the virus replication complex, alone or within the complex aligns with and traffics along microfilaments. Plant Physiol 138:1877–1895

Lucas WJ, Ham B-K, Kim J-K (2009) Plasmodesmata – bridging the gap between neighboring plant cells. Trends Cell Biol 19: 495-503

Macri F, Zancani M, Petrussa E, Dell'Antone P, Vianello A (1995) Pyrophosphate and H^+-pyrophosphatase maintain the vacuolar proton gradient in metabolic inhibitor-treated *Acer pseudoplatanus* cells. Biochim Biophys Acta 1229:323–328

Malec P, Ranaldi RA, Gabrys H (1996) Light-induced chloroplast movements in *Lemma trisulca*. Identification of the motile system. Plant Sci 120:127–137

McCurdy DW (1999) Is 2, 3-butanedione monoxime an effective inhibitor of myosin-based activities in plant cells? Protoplasma 209:120–125

Menzel D (1994) Dynamics and pharmacological perturbations of the endoplasmic reticulum in the unicellular green alga *Acetabularia*. Eur J Cell Biol 64:113–119

Mermall V, Post PL, Mooseker MS (1998) Unconventional myosins in cell movement, membrane traffic, and signal transduction. Science 279:527–533

Molchan TM, Valster AH, Hepler PK (2002) Actomyosin promotes cell plate alignment and late lateral expansion in *Tradescantia* stamen hair cells. Planta 214:683–693

Mooseker MS, Wolenski JS, Coleman TR, Hayden SM, Cheney RE, Espreafico E, Heintzelman MB, Peterson MD (1991) Structural and functional dissection of a membrane-bound mechanoenzyme: brush border myosin I. Curr Top Membr 38:31–55

Nagai R, Fukui S (1981) Differential treatment of *Acetabularia* with cytochalasin B and *N*-ethylmaleimide with special reference to their effects on cytoplasmic streaming. Protoplasma 109:79–89

Oiwa K, Kawakami T, Sugi H (1993) Unitary distance of actin–myosin sliding studied using an in vitro force-movement assay system combined with ATP iontophoresis. J Biochem 114:28–32

Oparka KJ (2004) Getting the message across: how do plant cells exchange macromolecular complexes? Trends Plant Sci 9:33–41

Patel JR, Diffee GM, Huang XP, Moss RL (1998) Phosphorylation of myosin regulatory light chain eliminates force-dependent changes in relaxation rates in skeletal muscle. Biophys J 74:360–368

Phillips RM, Altschuld RA (1996) 2, 3-butanedione 2-monoxime (BDM) induces calcium release from canine cardiac sarcoplasmic reticulum. Biochem Biophys Res Commun 229:154–157

Prokhnevsky AI, Peremyslov VV, Dolja VA (2005) Actin cytoskeleton is involved in targeting of a viral Hsp70 homolog to the cell periphery. J Virol 79: 14421–14428

Radford JE, White RG (1998) Localization of a myosin-like protein to plasmodesmata. Plant J 14:743–750

Radford JE, White RG (2001) Effects of tissue-preparation-induced callose synthesis on estimates of plasmodesma size exclusion limits. Protoplasma 216:47–55

RayChaudhuri A, Hait NC, Dasgupta S, Bhaduri TJ, Deb R, Majumder AL (1997) L-myo-inositol 1-phosphate synthase from plant sources. Plant Physiol 115:727–736

Reichelt S, Knight AE, Hodge TP, Baluska F, Samja J, Volkmann D, Kendrick-Jones J (1999) Characterization of the unconventional myosin VIII in plant cells and its localization at the post-cytokinetic cell wall. Plant J 19:555–567

Reisen D, Hanson MR (2007) Association of six YFP-myosin XI-tail fusions with mobile plant cell organelles BMC. Plant Biol 7:6

Robards AW, Kidwal P (1979) Cytochemical localization of phosphatase in differentiating secondary vascular cells. Planta 87:227–238

Roberts AG, Oparka KJ (2003) Plasmodesmata and the control of symplastic transport. Plant Cell Environ 26:103–124

Roopnarine O, Thomas DD (1996) Orientation of intermediate nucleotide states of indane dione spin-labeled myosin heads in muscle fibers. Biophys J 70:2795–2806

Safadi F, Mykles DL, Reddy ASN (1997) Partial purification and characterization of a Ca^{2+}-dependent proteinase from *Arabidopsis* roots. Arch Biochem Biophys 348:143–151

Salitz A, Schmitz K (1989) Influence of microfilament and microtubule inhibitors applied by immersion and microinjection on circulation streaming in the staminal hairs of *Tradescantia blossfeldiana*. Protoplasma 153:37–45

Sattarzadeh A, Krahmer J, Germain AD, Hanson MR (2009) A myosin XI tail domain homologous to the yeast myosin vacuole-binding domain interacts with plastids and stromules in *Nicotiana benthamiana*. Molec Plant 2:1351–1358

Schindler M, Jiang L (1986) Nuclear actin and myosin as control elements in nucleocytoplasmic transport. J Cell Biol 102:859–862

Schumaker KS, Gizinski MJ (1995) 1, 4-Dihydropyridine binding sites in moss plasma membranes. J Biol Chem 270:23461–23467

Seki M, Awata J-Y, Shimada K, Kashiyama T, Ito K, Yamamoto K (2003) Susceptibility of *Chara* myosin to SH reagents. Plant Cell Physiol 44:201–205

Shimmen T, Tazawa M (1983) Control of cytoplasmic streaming by ATP, Mg^{2+} and cytochalasin B in permeabilized Characeae cells. Protoplasma 115:18–24

Spudich JA (1994) How molecular motors work. Nature 372: 515–518

Spudich JA (2001) The myosin swinging cross-bridge model. Nat Rev Molec Cell Biol 2: 387–392

Su S, Liu Z, Chen C, Zhang Y, Wang X, Zhu L, Miao L, Wang X-C, Yuan M (2010) Cucumber Mosaic Virus movement protein severs actin filaments to increase the plasmodesmal size exclusion limit in tobacco. Plant Cell 22:1373–1387

Sugimoto Y, Tokunaga M, Takezawa Y, Ikebe M, Wakabayashi K (1995) Conformational changes of the myosin heads during hydrolysis of ATP as analyzed by X-ray solution scattering. Biophys J 68:29s–34s

Tilney LG, Cooke TJ, Connelly PS, Tilney MS (1991) The structure of plasmodesmata as revealed by plasmolysis, detergent extraction, and protease digestion. J Cell Biol 112:739–747

Tirlapur UK, König K (1999) Near-infrared femtosecond laser pulses as a novel non- invasive means for dye-permeation and 3D imaging of localised dye-coupling in the Arabidopsis root meristem. Plant J 20:363–370

Tominga T, Wayne R, Tung HYL, Tazawa M (1987) Phosphorylation-dephosphorylation is involved in Ca^{2+}-controlled cytoplasmic streaming of characean cells. Protoplasma 136:161–169

Tucker EB (1982) Translocation in the staminal hairs of *Setcreasea purpurea.* I. A study of cell ultrastructure and cell-to-cell passage of molecular probes. Protoplasma 113:193–201

Tucker EB (1987) Cytoplasmic streaming does not drive intercellular passage in staminal hairs of *Setcreasea purpurea*. Protoplasma 137:140–144

Tucker EB (1988) Inositol bisphosphate and inositol trisphosphate inhibit cell-to-cell passage of carboxyfluorescein in staminal hairs of *Setcreasea purpurea*. Planta 174:358–363

Tucker EB (1990) Calcium-loaded 1, 2-bis(2-aminophenoxy)ethane-*N*,*N*,*N*',*N*'-tetraacetic acid blocks cell-to-cell diffusion of carboxyfluorescein in staminal hairs of Setcreasea purpurea. Planta 182:34–38

Tucker EB (1993) Azide treatment enhances cell-to-cell diffusion in staminal hairs of *Setcreasea purpurea*. Protoplasma 174:45–49

Tucker EB, Boss WF (1996) Mastoparan-induced intracellular Ca^{2+} fluxes may regulate cell-to-cell communication in plants. Plant Physiol 111:459–467

Tucker EB, Tucker JE (1993) Cell-to-cell diffusion selectivity in staminal hairs of *Setcreasea purpurea*. Protoplasma 174:36–44

Tucker JE, Mauzerall D, Tucker EB (1989) Symplastic transport of carboxyfluorescein in staminal hairs of *Setcreasea purpurea* is diffusive and includes loss to the vacuole. Plant Physiol 90:1143–1147

Turner A, Wells B, Roberts K (1994) Plasmodesmata of maize root tips: structure and composition. J Cell Science 107:3351–3361

Uyeda TQ, Abramson PD, Spudich JA (1996) The neck region of the myosin motor domain acts as a lever arm to generate movement. Proc Natl Acad Sci USA 93:4459–4464

Verrucchia F, Hervé JC (1997) Reversible blockade of gap junctional communication by 2,3-butanedione monoxime in rat cardiac myocytes. Amer J Physiol 272:C875–C885

Vidali L, McKenna ST, Hepler PK (2001) Actin polymerization is essential for pollen tube growth. Mol Biol Cell 12:2534–2545

Vincente JAF, Vale MGP (1994) Proton transport by a fraction of endoplasmic reticulum and golgi membranes of corn roots: comparison with the plasma membrane and tonoplast H^+ pumps. Plant Sci 96:55–68

Volkmann D, Mori T, Tirlapur UK, Konig K, Fujiwara T, Kendrick-Jones J, Baluska F (2003) Unconventional myosins of the plant-specific class VIII: endocytosis, cytokinesis, plasmodesmata/pit-fields, and cell-to-cell coupling. Cell Biol Int 27:289–291

Walter N, Holweg CL (2008) Head-neck domain of *Arabidopsis* myosin XI, MYA2, fused with GFP produces F-actin patterns that coincide with fast organelle streaming in different plant cells. BMC Plant Biol 8:74

Wang ZY, Ramage RT, Portis AR Jr (1993) Mg^{2+} and ATP or adenosine 5′-[γ-thio]-triphosphate (ATPγS) enhances intrinsic fluorescence and induces aggregation which increases the activity of spinach rubisco activase. Biochim Biophys Acta 1202:47–55

Watanabe M (1993) Effects of 2, 3-butanedione monoxime on smooth-muscle contraction of guinea-pig portal vein. Pflugers Arch 425:462–468

White RG, Badelt K, Overall RL, Vesk M (1994) Actin associated with plasmodesmata. Protoplasma 180:169–184

Williamson RE (1975) Cytoplasmic streaming in *Chara*: a cell model activated by ATP and inhibited by cytochalasin B. J Cell Sci 17:655–668

Williamson RE (1992) Cytoplasmic streaming in Characean algae: mechanism, regulation by Ca^{2+}, and organization. In: Melkonian M (ed) Algal cell motility. Chapman, Hall, New York, pp 73–98

Xiao YF, McArdle JJ (1995) Effects of 2,3-butanedione monoxime on blood pressure, myocardial Ca^{2+} currents and action potentials of rats. Am J Hypertens 8:1232–1240

Xiong F, Gaon Y, Song P (1998) A long-lasting photorespiration in CO_2-free air, measured as the postirradiation CO_2 burst, indicates mobilization of storage photosynthates. Photosynthetica 35:107–119

Yamamoto K (2008) Plant myosins VIII, XI, and XIII. In: Coluccio LM (ed) Chapter 12 in Myosins: a superfamily of molecular motors. Springer, New York, pp 375–390

Zawadzki T, Fensom DS (1986) Transnodal transport of ^{14}C in Nitella flexilis. I. Tandem cells without applied pressure gradients. J Exp Bot 37:1341–1352

Zhang D, Wadsworth P, Hepler PK (1990) Microtubule dynamics in living dividing plant cells: confocal imaging of microinjected fluorescent brain tubulin. Proc Natl Acad Sci USA 87:8820–8824

Zhen R-G, Kim EJ, Rea PA (1994) Localization of cytosolically oriented maleimide-reactive domain of vacuolar H^+-pyrophosphatase. J Biol Chem 269:23342–23350

Zhu Y, Ideka SR (1993) 2,3-Butanedione monoxime blockade of Ca^{2+} currents in adult rat sympathetic neurons does not involve 'chemical phosphatase' activity. Neurosci Lett 155:24–28

Zurek B, Sanger JM, Sanger JW, Jockusch BM (1990) Differential effects of myosin-antibody complexes on contractile rings and circumferential belts in epitheloid cells. J Cell Sci 97:297–306